Retinal Sphingolipids and Their Very-Long-Chain Fatty Acid–Containing Species

Richard S. Brush, Julie-Thu A. Tran, Kimberly R. Henry, Mark E. McClellan, Michael H. Elliott, and Md Nawajes A. Mandal

Purpose. Recent evidence suggests that ceramide metabolism plays an important role in retinal photoreceptor cell survival and apoptosis. The purpose of this study was to characterize sphingolipids in the retina with special emphasis on the very-long-chain–containing saturated (VLC-FA) and polyunsaturated (VLC-PUFA) fatty acid–containing species. The VLC-FAs and VLC-PUFAs are synthesized by the ELOVL4 protein, which is involved in human Stargardt's macular dystrophy type 3 (STGD3).

Methods. Total lipids were extracted from retina and other tissues, and different sphingolipid classes were isolated and purified using various combinations of liquid- and solid-phase separation. Purified sphingolipids were analyzed by high-performance thin layer chromatography (HPTLC), gas chromatography (GC), and GC-MS (GC-mass spectrometry).

Results. Nonsialylated sphingolipids (NSLs) comprised ~3.5% of total retinal lipids of which 70% was sphingomyelin. Ceramide and glycosylceramides (GCs) constituted ≤1% of total retinal lipids. Gangliosides (GGs), on the other hand, comprised ~3.0% of total retinal lipids. Fatty acid analysis of retinal NSLs indicated an abundance of saturated fatty acids, with the presence of VLC-FAs but not of VLC-PUFAs beyond 24 carbons. However, GG had significant levels of unsaturated, polyunsaturated, and VLC-PUFAs. Retinal rod outer segments (ROS) contained ~1% each of NSL and GG, and their fatty acid profile was not very different from whole retinal NSL and GG, respectively.

Conclusions. Retina has a total of 6% to 7% fatty acids that are N-linked to a sphingosine, which would be 11 to 13 mole % in comparison to phospholipids. The presence of VLC-FAs and VLC-PUFAs in retinal sphingolipids indicates that they may play role in ELOVL4-mediated Stargardt 3. (*Invest Ophthalmol Vis Sci.* 2010;51:4422–4431) DOI:10.1167/iovs.09-5134

Sphingolipids are a family of membrane lipids that play important roles in the regulation of the fluidity and subdomain structure of the lipid bilayer—especially, lipid rafts.[1–4] They play crucial functional roles in membrane raft formation, receptor function, membrane conductance, cell–cell interactions, and internalization of pathogens.[2,5,6] Many of them, such as ceramide (CER), ceramide-1-phosphate (C1P), sphingosine (SP), and sphingosine-1-phosphate (S1P), are bioactive molecules that have been implicated in the regulation of cell growth, apoptosis, angiogenesis, vesicular trafficking, and a multitude of specific cell actions and responses.[6,7]

Aberrant sphingolipid metabolism is associated with inflammation, tumorigenesis, diabetes, and neurodegenerative disorders.[8–12] Sphingolipid metabolic defects that cause severe congenital or childhood-onset neurodegenerative diseases, such as Tay-Sachs disease, Fabry's disease, and Niemann-Pick disease, are often associated with blindness, indicating the importance of sphingolipid metabolism in retinal cells.[13–15] Patients with Farber's (acid ceramidase), Gaucher's (glucosylceramidase), Krabbe's (galactosylceramidase), and Niemann-Pick (sphingomyelinase) diseases lose vision due to retinal neuronal cell death.[16]

The processes of apoptosis, neuronal dedifferentiation, and neovascularization are integral to major retinal diseases including retinitis pigmentosa (RP), Stargardt's disease, Leber's congenital amaurosis (LCA), diabetic retinopathy, and age-related macular degeneration (AMD).[17–20] Recent evidence suggests a strong correlation between sphingolipid signaling and survival and homeostasis of photoreceptor and retinal pigment epithelial (RPE) cells: (1) CERs are mediators of retinal photoreceptor apoptosis, especially in oxidative stress–induced apoptosis[21]; (2) reducing the level of free CER through genetic manipulation rescues *Drosophila* photoreceptor cells from lethal mutations in the phototransduction genes[22]; (3) aberrant sphingolipid metabolism is reported in diabetic retinopathy[16]; (4) S1P signaling is involved in pathologic angiogenesis and choroidal neovascularization in the mouse retina[23,24]; and (5) mutations in the ceramide kinase–like (*CERKL*) gene, a gene predicted to be involved in CER metabolism, are involved in nonsyndromic retinal degeneration in human (RP26).[25–27] These results clearly support the functional role of sphingolipid signaling in retinal physiology and pathophysiology. However, very little is known about their metabolism, abundance, and composition in the retina. As the first step toward understanding their role(s) in the retina, we determined the abundance and molecular composition of retinal sphingolipids.

We have recently shown that the human Stargardt 3 (STGD3) retinal dystrophy protein ELOVL4 (elongation of very-long-chain fatty acid 4) is involved in biosynthesis of fatty acids with chain lengths >26 carbons.[28] These very-long-chain saturated, mono- and polyunsaturated fatty acids are present in tissues that express ELOVL4, such as retina, skin, and testis, but the specific role that they play is not well understood. Homozygous *Elovl4* knockout and knockin mice die after birth as a result of a peculiar skin barrier defect[29–31] resulting from a deficiency in a particular sphingolipid (*ω-O*-acylceramide) that contains very-long-chain fatty acids. As in the skin of these

From the Department of Ophthalmology, Dean A. McGee Eye Institute, University of Oklahoma Health Sciences Center, Oklahoma City, Oklahoma.

Supported by a Pediatric Ophthalmology grant from the Knight's Templar Eye Foundation (MNAM), an OU College of Medicine Alumni Association grant (MNAM), National Eye Institute Core Grant EY12190 for Vision Research, and National Center for Research Resources Grant RR17703 (MNAM).

Submitted for publication December 28, 2009; revised March 15, 2010; accepted March 17, 2010.

Disclosure: **R.S. Brush**, None; **J.-T.A. Tran**, None; **K.R. Henry**, None; **M.E. McClellan**, None; **M.H. Elliott**, None; **M.N.A. Mandal**, None

Corresponding author: Md Nawajes A. Mandal, Department of Ophthalmology, OUHSC, Dean A. McGee Eye Institute, 608 SL Young Boulevard, Oklahoma City, OK 73104; mmandal@ouhsc.edu.

Investigative Ophthalmology & Visual Science, September 2010, Vol. 51, No. 9

mice, there is a possibility that sphingolipids containing very-long-chain fatty acids are involved in ELOVL4-mediated retinal disease in humans. We, therefore, extended our studies to analyze, for the first time, retinal sphingolipids containing very-long-chain fatty acids.

Materials and Methods

Animal Care and Tissues

All procedures were performed according to the ARVO Statement for the Use of Animals in Ophthalmic and Vision Research and the University of Oklahoma Health Sciences Center (OUHSC) Guidelines for Animals in Research. All protocols were reviewed and approved by the Institutional Animal Care and Use Committees of the OUHSC and the Dean A. McGee Eye Institute (DMEI). Rat retinal tissues used in the study for lipid analysis were harvested after overnight dark adaptation. Other tissues such as brain, liver, skin, and testes were harvested at the same time, snap frozen in liquid N_2, and used for lipid extraction. Snap-frozen bovine retinas were purchased from Animal Technologies, Inc. (Tyler, TX). For preparation of ROS, we collected bovine retinas from freshly harvested eyes from a local abattoir (Country Home Meat Co., Edmond, OK).

Preparation of Bovine Retinal ROS

Freshly harvested bovine retinas were obtained from Country Home Meat Co. Three independent retina homogenates containing 12 to 16 retinas each were used to isolate the ROS fractions using methods described by Papermaster et al.,[32] with slight modification, as published earlier.[1] The band containing purified ROS was collected, diluted with homogenization buffer, and pelleted by centrifugation at 27,000*g* for 30 minutes at 4°C. The purity of the preparations was verified by SDS-PAGE (Supplementary Fig. S1, http://www.iovs.org/cgi/content/full/51/9/4422/DC1).

Total Lipid Extraction

Total lipids were extracted by first homogenizing rat tissues and bovine retinas in 1 mM diethylenetriaminepentaacetic acid (DTPA). Total lipids were then extracted from the aqueous suspension by the Bligh-Dyer method,[33] with minor modifications, as described previously by Martin et al.[1]

Individual Lipid Classes by 2D HPTLC

For analysis of phospholipid class composition and isolation of sphingomyelin (SM), the only NSL present in the phospholipid fraction, aliquots of total lipid extracts were spotted on normal-phase, high-performance thin-layer chromatography plates (HPTLC; Analtech, Newark, DE) after the plates had been treated with 3% magnesium acetate. For the separation of individual phospholipids, a two-dimensional (2D), three-solvent method was used, as published earlier.[1,34] The lipid spots were visualized with 2,7-dichlorofluorescein and five classes—namely, phosphatidylcholine (PC), phosphatidylethanolamine (PE), phosphatidylserine (PS), phosphatidylinositide (PI), and SM—were identified by comparison to commercially available standards and scraped from the plates. Lipids were extracted from the silica with chloroform-methanol-water 1:1:0.2 and were quantified by a lipid phosphorus assay.[35]

NSL Extraction

For NSL (CER and GC) extraction and analysis, total lipid extracts were first subjected to mild base hydrolysis (0.6 N NaOH in methanol-chloroform 1:1, at room temperature for 60 minutes with intermittent shaking) to remove the O-ester-bound fatty acids. The organic phase was then washed with water and Folch theoretical upper phase (chloroform-methanol-1 mM DTPA 3:48:47), dried under N_2, and suspended in 0.5 mL of *n*-hexane. Sphingolipid fractions were separated by solid-phase extraction according to the procedure described by Bodennec et al.,[36] with some modification. Lipid extracts in *n*-hexane were first applied to an aminopropyl silica gel column (100 mg/1.5 mL, Extract Clean SPE NH2; Alltech, Deerfield, IL) equilibrated with *n*-hexane. After the column was washed with 10 volumes of *n*-hexane (to remove most of the cholesterol), the fraction containing free CERs was eluted with chloroform-isopropanol 2:1 (fraction 1). The SM- and GC-containing fractions were then eluted with chloroform-methanol 1:1 and 1:2 (fraction 3) after the column was washed with diethyl ether containing 2% acetic acid (which removes the free fatty acids; fraction 2). Fraction 1 was re-eluted through an *n*-hexane-saturated column, first by *n*-hexane (discarded) and then by chloroform-isopropanol (2:1) to get rid of the remaining cholesterol. Fractions 1 and 3 containing the total NSL were then combined for fatty acid analyses and for separation into individual SM, CERs, or GC species by HPTLC.

Extraction of GGs

GGs were extracted from tissue homogenates, according to the procedure by Ladisch and Li.[37] Briefly, total lipid was obtained by three repeated extractions in chloroform-methanol (1:1). The extracts were reduced to approximately one third of the original volume by evaporation under N_2 and then stored overnight at −20°C. Clear GG-containing supernatant was removed after centrifugation and dried completely under N_2. This lipid extract was subjected to organic–aqueous partitioning by mixing with diisopropyl ether (DIPE), 1-butanol, and aqueous NaCl. Total GGs were collected after repeated partitioning and collecting the lower aqueous layer each time. They were then lyophilized and used for fatty acid analysis by GC coupled with either a flame ionization detector (GC-FID) or mass spectrometer (GC-MS).

HPTLC Analysis

The major sphingolipid/CER species were separated from isolated NSLs by HPTLC (Silica gel 60; Merck, Darmstadt, Germany) according to a procedure described elsewhere.[38] Total NSLs were dried, resuspended in 50 μL of chloroform-methanol (1:1), and spotted as a thin line on a 10 × 20-cm HPTLC plate. Individual CER species were separated with the following solvent sequences: (1) chloroform-methanol-water 40:10:1, to 4.0 cm; (2) the same solvent as in (1) up to 10.0 cm; (3) chloroform-methanol-acetic acid 47:2:0.5, to the top of the plate; and (4) *n*-hexane-diethyl ether-acetic acid 30:15:0.5, to the top of the plate. Lipids were visualized by charring (spraying with cupric acetate [0.165 M] in 7% phosphoric acid followed by heating at 100°C for 30 minutes). For fatty acid analysis, the HPTLC plate was stained with 2,7-dichlorofluoroscein and individual bands were scraped.

Fatty Acid Analysis

Fatty acid methyl esters (FAMEs) were prepared from total lipid extracts, NSLs, GGs, and individual NSL species by subjecting them to strong acid hydrolysis (16.6% HCl in methanol at 75°C overnight) as described in Agbaga et al.[28] FAMEs were analyzed by GC-FID, as described in Ford et al.[39] VLC-FAs (26 or more carbons) and VLC-PUFAs were quantified by GC-MS, as described elsewhere.[28]

Results

Relative Abundance of Sphingolipids in the Retina

To estimate the sphingolipid content in retinal tissue, we first measured the quantity of SM, the only amide-linked fatty acyl phospholipid. We determined the mole percent of SM by isolating major phospholipids by 2D TLC and measuring the inorganic phosphorus content (Supplementary Fig. S2, http://www.iovs.org/cgi/contents/full/51/9/4422/DC1).[1,34] In a comparative analysis of all the major phospholipids in major lipid- and/or sphingolipid-containing organs, we observed that retina (bovine and rat) contains 3.6 to 3.8 mole % SM of total the phospholipids (Fig. 1A). As shown in earlier work,[40] the retinal level of PC was found to be the highest (48–54 mole %) followed by PE (37–38 mole %; Fig. 1A). The levels of three other major phospholipids, PS, PI, and SM,

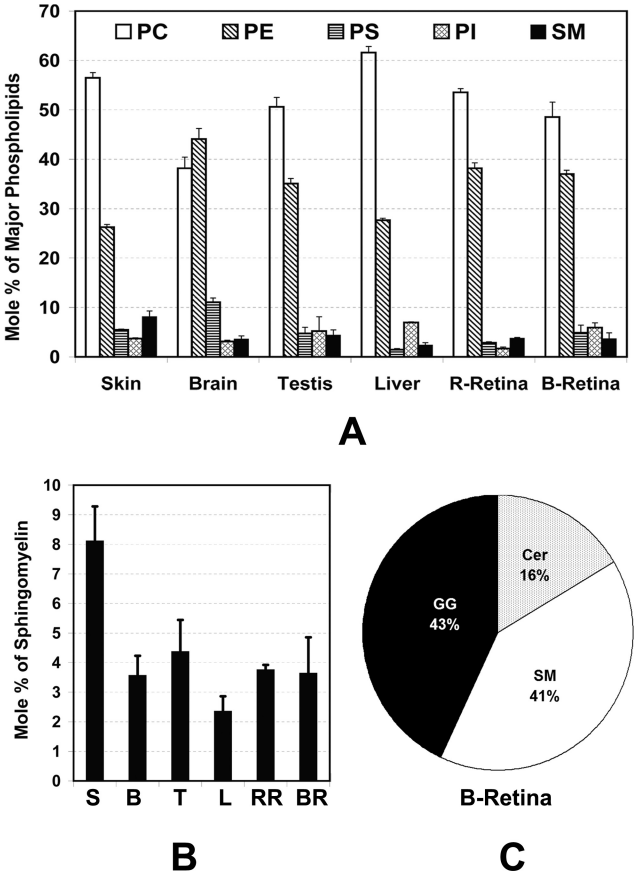

FIGURE 1. SM and phospholipid composition of various rat tissues and bovine retina. The phospholipid classes were resolved on a 2D HPTLC plate. Individual lipid spots were revealed with 2,7-dichlorofluorescein and identified by comparison to commercially available standards. Lipid extracts from each spot were quantified by measuring inorganic phosphorus content. Data are expressed as the mean mole percent ± SD, $n = 3$). (**A**) SM and major phospholipids and (**B**) SM in the different tissues. (**C**) Relative abundance of major sphingolipid species in bovine retina. R-Retina, rat retina; B-Retina, bovine retina; S, skin; B, brain; T, testis; L, liver; RR, rat retina; BR, bovine retina.

were almost the same (Fig 1A). This pattern of retinal phospholipid distribution is very similar to that distribution in testis but not brain (Fig. 1A). In brain, PE, not PC, was the most abundant phospholipid (44% PE vs. 38% PC; Fig. 1A). Also, the level of brain PS was significantly higher than in retina (11% vs. 3%–5%; Fig. 1A). However, the SM level of retina was very similar to that of brain (3.5%; Fig. 1B). Liver contained the lowest (2.3%) and skin the highest (8.1%) level of SM (Fig. 1B).

We then extracted the GG from bovine and rat retinas and rat brains. We also isolated NSLs (includes CER, GC, and SM) from retina and other rat tissues by solid-phase extraction. All these isolates, including the total SM isolated by 2D-TLC, as described earlier, were hydrolyzed with strong acid (to break the amide bonds) and analyzed by GC-FID to obtain fatty acid composition and nanomole and/or microgram values for each fatty acid. The values were then normalized with the protein quantity of the starting materials. Thus, the amount of fatty acids from NSLs ranged between 3.35% and 3.56% of total retinal fatty acid. Of that, the amount from SM was 2.40% to 2.53% (70%–80% of the NSL), and therefore the calculated amount for the free and simple glycosyl-CERs (CER+GC) was 0.96% to 1.01%. The fatty acids from GGs, on the other hand, ranged from 2.22% to 3.1% of the total retinal fatty acids.

In summary, 5.6% to 6.7% of fatty acids in the mammalian (bovine and rat) retina are linked to the amide moiety of an SP. As there is only one fatty acid attached to one molecule of sphingolipid, the mole percent of retinal sphingolipids range from 11.2% 13.4% in relation to phospholipids, which have two fatty acids per molecule. The percentage of three major groups of amide-containing lipids in the retina was 43% GGs, 41% SMs, and 16% simple and glucosyl CERs (Fig. 1C).

We then analyzed bovine retinal ROS. We found that fatty acid levels of NSLs in bovine ROS varied from 0.8% to 1.4% of total ROS fatty acids and that GG varied from 0.9% to 1.8%. Therefore, N-linked fatty acids in bovine ROS varied from 1.7% to 3.2% of total fatty acids (TFAs), which is equivalent to 3.4 to 6.4 mole % of phospholipids.

NSL Classes in the Retina

By solid-phase extraction, the NSL fractions containing CERs, GCs, and SMs were pooled and separated by HPTLC. In bovine and rat retina, we recognized three to four species of nonhydroxy-CER, two to four species of α-OH CER, two to four species of GC, and two species of SM (Fig. 2A). In a comparative analysis, we detected a similar pattern of CER distribution in rat brain, except that the level of GCs was substantially higher than that in the retina (Fig. 2A). Skin contained much higher amounts of free CER species and had only one major type of SM, whereas brain and retina had two major species of SM (Fig. 2A).

We then grouped the species of retinal CERs into seven classes, S1 to S7. S1 contains mostly nonhydroxy- and ω-hydroxy-acylceramide, S2 contains mostly α-hydroxy CER, S3 most likely represents ω-hydroxy glucosylceramides,[31,38] S4 contains gluco- or glycosylceramides, S5 and S6 contain some unidentified and more polar head–containing CERs that may represent some species of GC, and S7 represents SM. Total nanomoles of fatty acids in each fraction were determined by GC-FID analysis and used to calculate the relative abundance of these species in bovine and rat retina (Fig. 2B). SM constitutes 64% to 72% (S7), free CER constitutes 15% to 18% (S1 and S2), and others (GCs) constitute 12% to 22% (S3–S6) of the NSLs from bovine and rat retina (Fig. 2B).

NSL Fatty Acid Composition of Retina and Comparison with Other Tissues

In Table 1, we compared the sphingolipid fatty acid composition of bovine and rat retina and four other rat tissues: brain, liver, skin, and testis. The retina contained the highest level of saturated fatty acids (86%–89%), followed by liver (80%), brain (75%), skin (66%), and testis, which contained the lowest quantity of saturated fatty acids (60%). The reverse is true of the mono- and polyunsaturated fatty acids: The testis had the highest (40%) quantity followed by skin (34%), brain (25%), liver (20%), and retina (11%; Table 1).

When we analyzed, in detail, the individual fatty acid species, we observed that 44% to 63% of retinal CERs contained 18:0 and 11% to 19% contained 16:0. Brain CERs also contained two major species of saturated FA, 18:0 (41%) and 24:0 (18%). In testis, the major two species were the same as in retina, but the relative abundance was reversed, with levels of 16:0 being higher than 18:0 (31% and 19%, respectively). Liver NSL comprised three major species of saturates, 16:0, 18:0, and 24:0, at almost equal quantities (20%–25%). Skin NSL contained 20% of 16:0 and almost equal quantities each of 20:0, 22:0, and 24:0 (12%–13%). Skin had the lowest level of 18:0 among all the tissues tested (8%; Table 1).

Among the monounsaturates, brain had the highest levels of 24:1 (17%), whereas testis was enriched in 18:1 (12%), and the skin with both (8%–9% each). Retina contained a low quantity

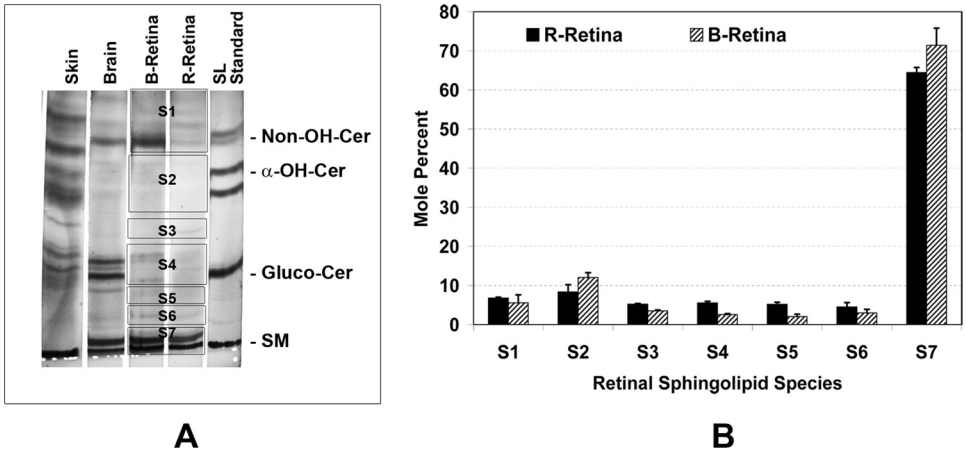

Figure 2. Separation and identification of sphingolipid classes. (**A**) Representative separation of sphingolipids by HPTLC. After mild base hydrolysis, total lipids were separated into different fractions by solid-phase extraction with aminopropyl-silica gel columns. Fractions 1 and 3 containing sphingolipids (SLs) and CER (Cer) were combined and resolved on an HPTLC plate, along with CER standards (SL Standard). Retinal CERs were divided into seven individual groups (S1–S7). (**B**) The fractions of individual groups were determined from their fatty acid content obtained by GC analysis. Replicate samples were run on separate plates under the same conditions as shown in (**A**) for fatty acid quantification. Individual bands visualized with 2,7-dichlorofluorescein were scraped and lipids were extracted and analyzed by GC-FID. Data are expressed the mean mole percent ± SD (n = 3). R-Retina, rat retina; B-Retina, bovine retina.

of monounsaturates (6%–7% compared with 21% in brain) and almost equivalent distributions of the species 16:1 and 24:1 (1%–2% each; Table 1).

Retinal sphingolipids contained the lowest levels of n6 polyunsaturated fatty acids (1.4%–1.7%). The highest levels were found in testis (17%), followed by that in skin (10%; Table 1). In the brain and retina, the most abundant n6 species was arachidonic acid (20:4n6). In the other tissues, linoleic acid (18:2n6) was most abundant, followed by arachidonic acid. The level of n3 polyunsaturated fatty acids was higher in retina (3%–4%) than in brain (1.5%) and skin (1.7%), and the level was comparable to that in testis (4%) and liver (4.5%; Table 1). In most of the tissues, the most abundant species of n3 fatty acid was DHA (22:6n3). The ratio of n6/n3 was distinctly

Table 1. Fatty Acid Composition of NSLs from Retina and Other Tissue

Fatty Acid	B-Retina	R-Retina	Brain	Testis	Liver	Skin
14:0	0.39 ± 0.07	0.41 ± 0.07	0.37 ± 0.20	0.49 ± 0.06	0.51 ± 0.14	0.50 ± 0.11
16:0	11.30 ± 0.61	19.05 ± 0.45	5.70 ± 1.51	31.39 ± 1.38	20.74 ± 1.23	20.49 ± 0.35
18:0	62.69 ± 1.43	44.74 ± 0.83	40.68 ± 9.08	19.39 ± 4.99	23.34 ± 9.72	7.81 ± 0.31
20:0	5.72 ± 0.02	9.93 ± 0.96	4.43 ± 0.30	2.00 ± 0.86	1.92 ± 0.19	13.04 ± 0.94
22:0	4.69 ± 0.17	5.38 ± 0.55	6.22 ± 1.32	2.80 ± 0.96	8.32 ± 2.21	12.77 ± 0.79
24:0	4.34 ± 0.28	6.26 ± 0.75	17.64 ± 2.84	3.95 ± 1.37	24.98 ± 6.03	11.72 ± 0.92
Total saturate	**89.12 ± 2.57**	**86.28 ± 3.90**	**75.04 ± 15.25**	**60.02 ± 9.63**	**79.82 ± 19.52**	**66.33 ± 3.41**
16:1	0.70 ± 0.15	1.98 ± 0.09	0.65 ± 0.31	2.27 ± 0.34	2.62 ± 1.35	2.42 ± 0.20
18:1	1.73 ± 0.35	1.01 ± 0.49	1.57 ± 0.08	11.67 ± 2.40	2.02 ± 1.17	8.64 ± 1.48
20:1	0.70 ± 0.15	0.73 ± 0.25	0.59 ± 0.29	0.21 ± 0.15	0.74 ± 0.11	1.28 ± 0.12
22:1	1.24 ± 0.36	0.93 ± 0.08	1.11 ± 0.27	0.79 ± 0.18	2.42 ± 0.86	1.70 ± 0.16
24:1	1.77 ± 0.96	2.51 ± 0.11	17.07 ± 7.31	3.90 ± 1.85	5.04 ± 1.00	7.77 ± 0.59
Total monounsaturate	**6.14 ± 1.97**	**7.16 ± 1.03**	**20.98 ± 8.26**	**18.85 ± 4.92**	**12.85 ± 4.49**	**21.80 ± 2.54**
18:2n6	0.25 ± 0.06	0.59 ± 0.11	0.18 ± 0.03	10.46 ± 2.90	1.63 ± 0.79	7.89 ± 0.78
18:3n6	ND	ND	ND	<0.05	ND	0.17 ± 0.01
20:2n6	ND	ND	ND	0.16 ± 0.02	ND	0.49 ± 0.05
20:3n6	0.40 ± 0.17	ND	1.04 ± 0.73	0.28 ± 0.05	<0.05	0.26 ± 0.02
20:4n6	0.85 ± 0.05	0.85 ± 0.35	1.17 ± 0.56	2.95 ± 1.68	1.19 ± 0.84	1.14 ± 0.11
22:4n6	0.12 ± 0.10	ND	0.14 ± 0.02	0.51 ± 0.23	ND	0.24 ± 0.02
22:5n6	0.07 ± 0.07	ND	ND	2.71 ± 1.37	ND	ND
Total n6	**1.69 ± 0.46**	**1.44 ± 0.46**	**2.53 ± 1.34**	**17.08 ± 6.27**	**2.82 ± 1.62**	**10.19 ± 0.98**
18:3n3	0.56 ± 0.02	0.68 ± 0.20	0.24 ± 0.04	0.81 ± 0.04	0.54 ± 0.16	0.58 ± 0.02
20:5n3	0.28 ± 0.06	ND	0.27 ± 0.11	0.37 ± 0.13	1.60 ± 1.03	0.43 ± 0.10
22:5n3	0.20 ± 0.11	ND	ND	0.60 ± 0.33	0.05 ± 0.00	0.15 ± 0.02
22:6n3	2.00 ± 0.23	3.34 ± 0.20	0.94 ± 0.27	2.23 ± 1.15	2.29 ± 0.55	0.53 ± 0.03
Total n3	**3.05 ± 0.41**	**4.02 ± 0.40**	**1.45 ± 0.42**	**4.02 ± 1.66**	**4.49 ± 1.74**	**1.69 ± 0.18**
n6+n3	**4.74 ± 0.87**	**5.46 ± 0.86**	**3.98 ± 1.75**	**21.09 ± 7.92**	**7.31 ± 3.45**	**11.87 ± 1.16**
n6/n3	**0.56 ± 0.13**	**0.36 ± 0.06**	**1.73 ± 0.68**	**4.11 ± 0.78**	**0.82 ± 0.48**	**6.05 ± 0.64**

Relative mole percent (mean ± SD; n = 3) of fatty acids from total NSL extracted from bovine retina, rat retina, and rat brain, testis, liver, and skin. Totals are indicated by bold type. B-Retina, bovine retina; R-Retina, rat retina.

different in these tissues: The lowest was in retina (0.36–0.56) and the highest was in skin (6.05; Table 1).

Fatty Acid Composition of GGs and NSLs from Retina and ROS

We observed earlier that GGs make up almost half of the total sphingolipids in the retina (Fig 1C). We analyzed the fatty acid composition of retinal (bovine) GGs and compared the results with those of whole retinal fatty acids (TFAs) and NSLs (Table 2). Unlike retinal NSLs, the GGs contained almost equal levels of saturated and unsaturated fatty acids, which were similar to TFAs (Table 2, Column TFA). Like total retina and NSLs, the two major saturates in retinal GGs were 18:0 (34%) and 16:0 (14%). In TFAs the levels of 18:0 and 16:0 were 26% and 26%, and in NSLs they were 63% and 11%, respectively. The 18:1 was the major monounsaturate in retinal GGs, very similar to TFA (Table 2). Retinal GGs contained a significantly higher quantity of n6 fatty acids (21% in comparison to 14% in TFAs and 1.69% in NSLs), and arachidonic acid was the major species (Table 2). The n3 fatty acid content was also significantly higher than that of NSLs (16% vs. 3%), with DHA being the most abundant. The n6/n3 ratio was 1.3 in the GG fraction and 0.73 and 0.56 in TFAs and NSLs, respectively. Brain is the other organ in mammals known to contain higher amounts of GGs. We therefore included rat brain for GG analysis, to have a comparative view of retinal GG composition (Table 2, last column). It was very similar to brain GG composition. The GG species that showed a difference between retina and brain was that with 18:1 (19% vs. 11%) and 22:5n6 (0.51% vs. 3.3%) fatty acids.

We then analyzed bovine ROS for NSL and GG fatty acid composition, each of which contributes approximately 1% of the total retinal fatty acids (Table 2). Saturated fatty acids make up 99% of ROS NSLs, and the relative distribution of species was very similar to that in whole retinal NSLs (Table 2). Unsaturated NSL species contributed <1% of ROS NSLs. GGs, on the other hand, contained significantly higher levels of unsaturated fatty acids in the ROS (40%). GGs with saturated fatty acids composed ~60% of ROS GGs, and the relative distribution of the species was very similar to that of ROS NSLs and total retinal NSLs (Table 2). Among the major unsaturated species, DHA contributed approximately 22%, arachidonic acid 6%, linoleic acid 4%, docosapentaenoic acid 3%, and docosatetraenoic acid 2.5% (Table 2) in the ROS GGs.

Fatty Acid Composition of Seven NSL Classes in the Retina

As shown in Figure 2A, we grouped retinal NSLs (separated by HPTLC) into 7 different categories and subjected them to fatty acid analysis by GC-FID. As obtained from total NSL analysis (Tables 1, 2), fatty acid analysis of S1 to S7 CERs also showed an abundance of saturated fatty acids ranging from 70% (S1) to 96% (S7) (Table 3), with 18:0 being the most abundant species. Inversely, S7 contained the lowest level of unsaturated fatty acids (4%–5%, mono+poly), and S1 contained the highest (25%–35%; Table 3). Among individual species of mono- and polyunsaturated fatty acids, S1 contained higher levels of 22:1 (6%) and 22:6n3 (7%), whereas the GC species contained higher levels of eicosapentaenoic acid (EPA, 20:5n3; Table 3).

Very-Long-Chain Fatty Acids in Retinal Sphingolipids

Retinal photoreceptors are known to contain high levels of very-long-chain polyunsaturated fatty acids (VLC-PUFA; carbons > 26) in PC.[41] We detected traces of VLC-FAs in the TFAs

TABLE 2. Fatty Acid Composition Bovine Retina and ROS Fractions: TFAs, NSLs, and GGs

Fatty Acid	Whole Retina			ROS			Rat Brain
	TFA	NSL	GG	TFA	NSL	GG	GG
14:0	0.44 ± 0.05	0.39 ± 0.07	0.21 ± 0.04	0.35 ± 0.02	0.66 ± 0.1616	ND	0.08 ± 0.00
16:0	26.24 ± 1.66	11.30 ± 0.61	13.69 ± 2.22	20.90 ± 0.81	17.04 ± 3.99	9.95 ± 0.93	10.71 ± 0.15
18:0	26.46 ± 1.83	62.69 ± 1.43	34.09 ± 3.10	23.65 ± 0.72	68.29 ± 3.63	42.49 ± 1.28	36.24 ± 0.76
20:0	0.40 ± 0.06	5.72 ± 0.02	1.61 ± 0.33	0.24 ± 0.01	5.75 ± 0.50	4.18 ± 0.31	0.98 ± 0.08
22:0	0.24 ± 0.04	4.69 ± 0.17	0.94 ± 0.15	0.11 ± 0.01	3.95 ± 0.32	2.41 ± 0.23	0.67 ± 0.07
24:0	0.18 ± 0.02	4.34 ± 0.28	0.47 ± 0.04	0.09 ± 0.01	3.49 ± 0.59	1.07 ± 0.07	0.97 ± 0.11
Total saturate	**53.96 ± 3.65**	**89.12 ± 2.57**	**51.01 ± 5.88**	**45.34 ± 1.59**	**99.19 ± 9.18**	**60.10 ± 2.82**	**49.65 ± 1.17**
16:1	0.71 ± 0.04	0.70 ± 0.15	0.81 ± 0.03	0.50 ± 0.04	0.03 ± 0.05	0.04 ± 0.01	0.49 ± 0.01
18:1	10.91 ± 0.61	1.73 ± 0.35	11.06 ± 0.46	6.53 ± 0.46	0.13 ± 0.03	3.98 ± 0.04	19.24 ± 1.42
20:1	0.27 ± 0.01	0.70 ± 0.15	0.24 ± 0.03	0.16 ± 0.01	ND	0.14 ± 0.01	0.98 ± 0.22
22:1	0.11 ± 0.04	1.24 ± 0.36	0.14 ± 0.01	0.07 ± 0.02	0.16 ± 0.08	0.17 ± 0.05	0.21 ± 0.02
24:1	0.08 ± 0.02	1.77 ± 0.96	0.23 ± 0.03	0.03 ± 0.01	0.17 ± 0.09	0.62 ± 0.08	1.25 ± 0.20
Total monounsaturate	**12.09 ± 0.72**	**6.14 ± 1.97**	**12.48 ± 0.56**	**7.30 ± 0.55**	**0.49 ± 0.25**	**4.95 ± 0.24**	**22.17 ± 1.87**
18:2n6	0.96 ± 0.13	0.25 ± 0.06	1.99 ± 0.12	0.78 ± 0.05	ND	0.32 ± 0.03	0.77 ± 0.04
18:3n6	0.14 ± 0.03	ND	0.12 ± 0.02	0.24 ± 0.02	0.12 ± 0.07	0.04 ± 0.01	>0.05
20:2n6	0.12 ± 0.03	ND	0.20 ± 0.01	0.11 ± 0.01	ND	0.03 ± 0.01	0.11 ± 0.01
20:3n6	0.79 ± 0.08	0.40 ± 0.17	0.93 ± 0.05	0.65 ± 0.07	ND	0.47 ± 0.03	0.50 ± 0.01
20:4n6	7.61 ± 0.51	0.85 ± 0.05	11.38 ± 0.60	5.94 ± 0.34	ND	6.20 ± 0.03	10.84 ± 0.31
22:4n6	2.20 ± 0.39	0.12 ± 0.10	2.72 ± 0.21	2.62 ± 0.44	ND	2.45 ± 0.02	2.25 ± 0.06
22:5n6	2.49 ± 1.08	0.07 ± 0.07	3.32 ± 0.38	4.12 ± 1.47	ND	3.2 ± 1.0	0.51 ± 0.08
Total n6	**14.32 ± 2.25**	**1.69 ± 0.46**	**20.66 ± 1.39**	**14.46 ± 2.4**	**0.12 ± 0.07**	**12.76 ± 1.21**	**14.98 ± 0.56**
18:3n3	0.12 ± 0.00	0.56 ± 0.02	0.17 ± 0.02		ND	ND	0.08 ± 0.0
20:5n3	0.02 ± 0.01	0.28 ± 0.06	0.17 ± 0.02	0.03 ± 0.01	ND	ND	0.08 ± 0.00
22:5n3	0.95 ± 0.09	0.20 ± 0.11	0.66 ± 0.06	0.47 ± 0.09	ND	0.66 ± 0.05	0.12 ± 0.00
22:6n3	18.67 ± 1.92	2.00 ± 0.23	15.02 ± 1.05	32.39 ± 3.10	ND	21.54 ± 3.82	12.99 ± 0.89
Total n3	**19.63 ± 2.06**	**3.05 ± 0.41**	**15.85 ± 1.13**	**32.88 ± 3.23**	**ND**	**22.20 ± 3.87**	**13.19 ± 0.89**
n6+n3	**33.95 ± 4.31**	**4.74 ± 0.87**	**36.51 ± 2.52**	**47.34 ± 5.63**	**0.12 ± 0.07**	**34.99 ± 5.12**	**28.17 ± 2.45**
n6/n3	**0.73 ± 0.11**	**0.56 ± 0.13**	**1.31 ± 0.08**	**0.45 ± 0.11**	**ND**	**0.59 ± 0.14**	**1.14 ± 0.05**

Relative mole percent (mean ± SD; $n = 3$). Rat brain GG was included for comparison. Totals are indicated by bold type.

TABLE 3. Fatty Acid Composition of Different Sphingolipid Fractions of Bovine Retina

Fatty Acid	S1	S2	S3	S4	S5	S6	S7
14:0	1.78 ± 1.26	0.45 ± 0.14	1.41 ± 0.45	1.16 ± 0.03	1.02 ± 0.29	0.76 ± 0.17	0.20 ± 0.03
16:0	30.61 ± 9.56	8.74 ± 1.40	24.58 ± 2.71	16.75 ± 6.24	19.72 ± 5.13	15.31 ± 3.54	9.63 ± 1.11
18:0	34.00 ± 4.44	61.45 ± 4.59	52.63 ± 3.77	45.99 ± 3.75	48.28 ± 3.98	51.29 ± 3.61	70.37 ± 2.24
20:0	1.12 ± 0.44	6.12 ± 1.14	2.33 ± 0.59	4.14 ± 1.63	2.29 ± 0.47	4.98 ± 1.35	6.41 ± 0.35
22:0	1.29 ± 0.56	4.05 ± 0.81	1.86 ± 0.49	6.05 ± 2.21	2.63 ± 0.85	4.47 ± 0.77	5.68 ± 0.23
24:0	1.80 ± 0.31	3.12 ± 0.68	1.59 ± 0.34	7.54 ± 2.87	2.38 ± 1.08	3.70 ± 0.64	3.83 ± 2.15
Total saturate	**70.60 ± 16.56**	**83.94 ± 8.77**	**84.40 ± 8.35**	**81.64 ± 16.73**	**76.32 ± 11.80**	**80.51 ± 10.08**	**96.12 ± 6.11**
16:1	2.99 ± 1.23	0.89 ± 0.47	4.26 ± 0.84	4.67 ± 2.02	7.90 ± 2.88	7.28 ± 2.42	0.20 ± 0.12
18:1	3.95 ± 1.90	2.44 ± 1.14	1.73 ± 0.79	0.52 ± 0.17	ND	1.30 ± 0.95	0.29 ± 0.06
20:1	1.31 ± 0.44	0.90 ± 0.25	2.09 ± 0.57	4.29 ± 1.68	5.88 ± 3.51	4.22 ± 2.11	0.12 ± 0.07
22:1	6.37 ± 3.65	6.45 ± 1.71	1.75 ± 0.70	3.85 ± 0.10	2.14 ± 0.24	1.19 ± 0.32	0.30 ± 0.02
24:1	2.10 ± 0.23	1.86 ± 0.95	0.25 ± 0.14	0.29 ± 0.10	<0.1	0.42 ± 0.15	1.85 ± 0.34
Total monounsaturate	**16.72 ± 8.45**	**12.54 ± 4.51**	**10.08 ± 3.05**	**13.62 ± 4.06**	**15.98 ± 6.78**	**14.41 ± 5.95**	**2.76 ± 0.61**
18:2n6	0.81 ± 0.21	0.46 ± 0.25	0.27 ± 0.26	ND	ND	<0.1	<0.1
18:3n6	<0.1	<0.1	0.71 ± 0.18	0.64 ± 0.20	1.13 ± 0.38	0.96 ± 0.35	<0.1
20:2n6	<0.1	ND	ND	ND	ND	ND	ND
20:3n6	0.35 ± 0.18	<0.1	ND	ND	ND	ND	0.16 ± 0.07
20:4n6	0.80 ± 0.30	1.07 ± 0.47	0.75 ± 0.17	ND	ND	0.15 ± 0.04	<0.1
22:4n6	0.75 ± 0.28	<0.1	<0.1	ND	ND	ND	ND
22:5n6	0.99 ± 0.20	<0.1	<0.1	ND	ND	ND	ND
Total n6	**3.70 ± 1.38**	**1.84 ± 1.13**	**1.82 ± 0.71**	**0.64 ± 0.20**	**1.13 ± 0.38**	**1.17 ± 0.82**	**0.39 ± 0.28**
18:3n3	0.41 ± 0.16	0.59 ± 0.08	0.67 ± 0.15	0.91 ± 0.14	0.76 ± 0.17	0.90 ± 0.18	0.62 ± 0.07
20:5n3	1.24 ± 0.71	0.53 ± 0.35	2.43 ± 1.00	3.28 ± 1.04	5.88 ± 2.69	3.27 ± 0.85	0.10 ± 0.05
22:5n3	0.12 ± 0.08	0.14 ± 0.01	ND	ND	ND	ND	ND
22:6n3	7.21 ± 3.33	0.94 ± 0.24	1.32 ± 0.55	<0.1	ND	0.24 ± 0.12	<0.1
Total n3	**8.98 ± 4.28**	**2.20 ± 0.69**	**4.42 ± 1.69**	**4.24 ± 1.32**	**6.64 ± 2.86**	**4.40 ± 1.15**	**0.76 ± 0.18**
n6+n3	**12.68 ± 5.66**	**4.04 ± 1.82**	**6.24 ± 2.40**	**4.88 ± 1.52**	**7.73 ± 3.24**	**5.57 ± 1.97**	**1.11 ± 0.46**
n6/n3	**0.42**	**0.84**	**0.41**	**0.15**	**0.17**	**0.27**	**0.51**

Relative mole percent (mean ± SD; $n = 4$) of different fatty acids in each class of retinal NSLs were calculated by analyzing the fatty acid methyl esters on a GC after separation of total NSLs using HPTLC. Scraped spots from the plate were subjected to extraction, and the fatty acids liberated by treatment with strong acid (16% HCl in methanol). Totals are indicated by bold type.

from bovine, rat, and mouse retina (Mandal et al., unpublished data, 2009). We therefore predicted that retinal sphingolipids also contain VLC-FAs and VLC-PUFAs. In a careful analysis of the purified SM fraction (using 2D-TLC) from retinal lipids, we did not detect any VLC-PUFAs (Fig. 3A). Since the retina contains the highest levels of VLC-PUFAs of any mammalian tissue analyzed thus far,[42,43] their absence in SM was unexpected. We then analyzed the PC fraction from the same 2D plate, and, as expected, we detected significant levels of VLC-PUFAs (Fig. 3A). To be sure that we were not losing VLC-PUFA-containing SM in our extraction and purification procedure, we analyzed SM from rat testis, as it is known to contain VLC-PUFAs.[44,45] Much as in retinal PC, we detected high levels of VLC-PUFA in the SM fraction of rat testis—mostly two n6 species: 28:4n6 and 30:5n6 (Fig. 3B)—indicating that VLC-PUFA-containing SM was not lost during extraction.

We then asked whether the six NSL classes other than SM might contain VLC-PUFAs, which includes nonhydroxy-, α-, and ω-hydroxy CERs and gluco- and galactosylceramides. As in the SM fraction, we did not detect any VLC-PUFAs in the total retinal NSL by using GC-MS (*m/z* ratios 79.1, 108.1, and 150.1 in SIM [selected ion monitoring] mode; Fig. 3C). We did, however, observe many peaks with mass fragments consistent with cholesterol derivatives (Fig. 3C). The longest chain PUFAs found in the retinal NSLs was 24:4n6 (Fig. 3C). The testis NSLs (the positive control), on the other hand, had easily detectable levels of a variety of VLC-PUFAs (Fig. 3C). We therefore conclude that retinal NSLs do not contain detectable levels of VLC-PUFAs.

GGs, on the other hand, contained higher levels of unsaturated and polyunsaturated fatty acids (Table 2). GC-MS analysis indeed showed various species of VLC-PUFAs in the GG fraction of bovine retina (Fig. 4A). As shown in Figure 4B, we calculated the relative quantity of various VLC-PUFA species in retinal GGs, and it ranged from 0.02 to 0.2 mole % of total GGs. The total VLC-PUFA-containing GGs in retina accounted for ~0.4 mole % of the total GG.

We then analyzed for very-long-chain saturated fatty acid-containing CERs (pool of 26:0, 28:0, and 30:0) in the retina and ROS, in retina and ROS GGs, and in other tissues. The mole percent of VLC-FA is calculated from the TFAs of that particular isolate. As shown in Figure 4C, the relative mole percent of VLC-FA CERs (26:0 + 28:0 + 30:0) varied from 0.1% to 1.5% of total NSLs in different tissues, where testis had the lowest level (0.1%) and skin had the highest (1.5%). Retinal VLC-FA CERs ranged from 210 to 240 picomoles/nanomole of total NSL (i.e., 0.2 mole %; Fig. 4C). Retinal ROS, on the other hand, had over 0.4 mole % of VLC-FA CERs of total NSL (Fig. 4C). The GGs from total retina and retinal ROS contained 0.1 and 0.07 mole % of VLC-FAs of the total GG fatty acids, respectively (Fig. 4C). The ratio of the VLC-FA species 26:0, 28:0, and 30:0 in different tissues were as follows: skin (76:13:11), brain (98:2:0), testis (73:24:3), liver (77:23:1), retina (83:13:4), ROS (81:17:2), retina-GG (78:18:4), and ROS-GG (74:18:8).

DISCUSSION

Sphingolipids constitute a small fraction of membrane lipids in all cells, with higher levels in neural tissues and skin.[46–48] Although they represent a minor group of cellular lipids, sphingolipids have great complexity in their structure and in the regulation of their synthesis, which is currently not well understood. The complex nature of these molecules may explain why general information concerning them is scarce. The retina is a neural tissue, and it is now established that sphingolipid metabolism plays important roles in retinal cell death and survival.[16,21,22,27] However, very little information on retinal

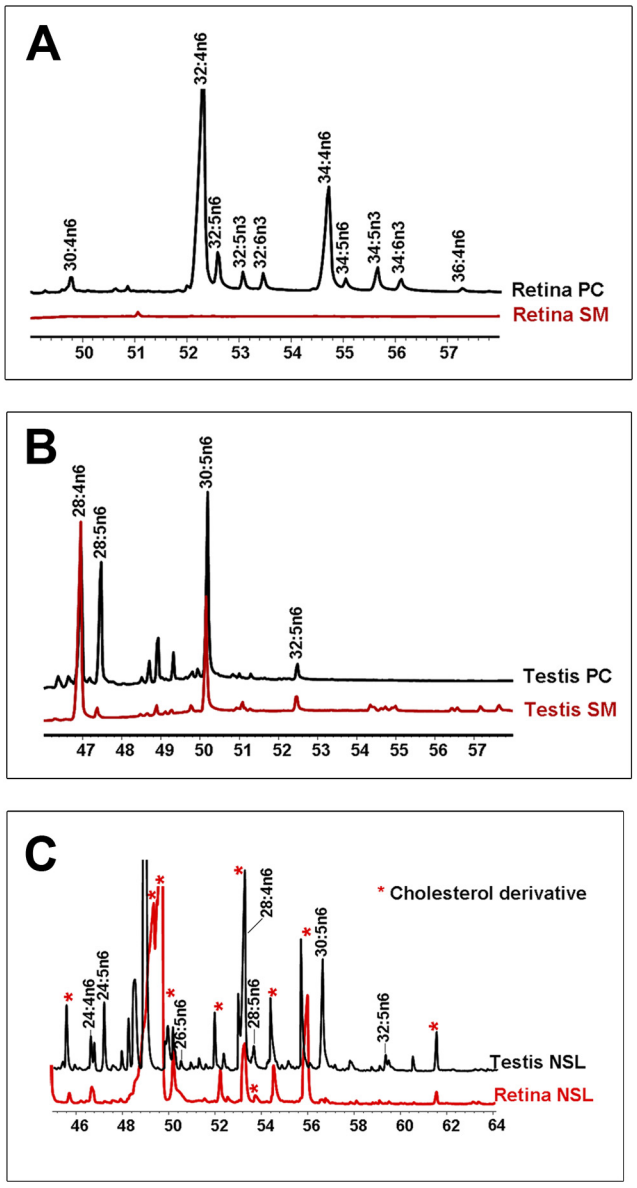

FIGURE 3. Analysis of VLC-PUFAs by GC-MS, which allowed identification of the VLC-PUFAs derived from samples of bovine retinal SM, phosphatidylcholine PC, and NSL. Rat testis SM, PC, and NSL were used as control samples. The PUFA response values were obtained by using the *m/z* ratios 79.1, 108.1, and 150.1, respectively, in SIM mode. (**A**) Bovine retinal PC and bovine retinal SM (*red*); (**B**) rat testis PC and rat testis SM (*red*); (**C**) rat testis NSL and bovine retinal NSL (*red*).

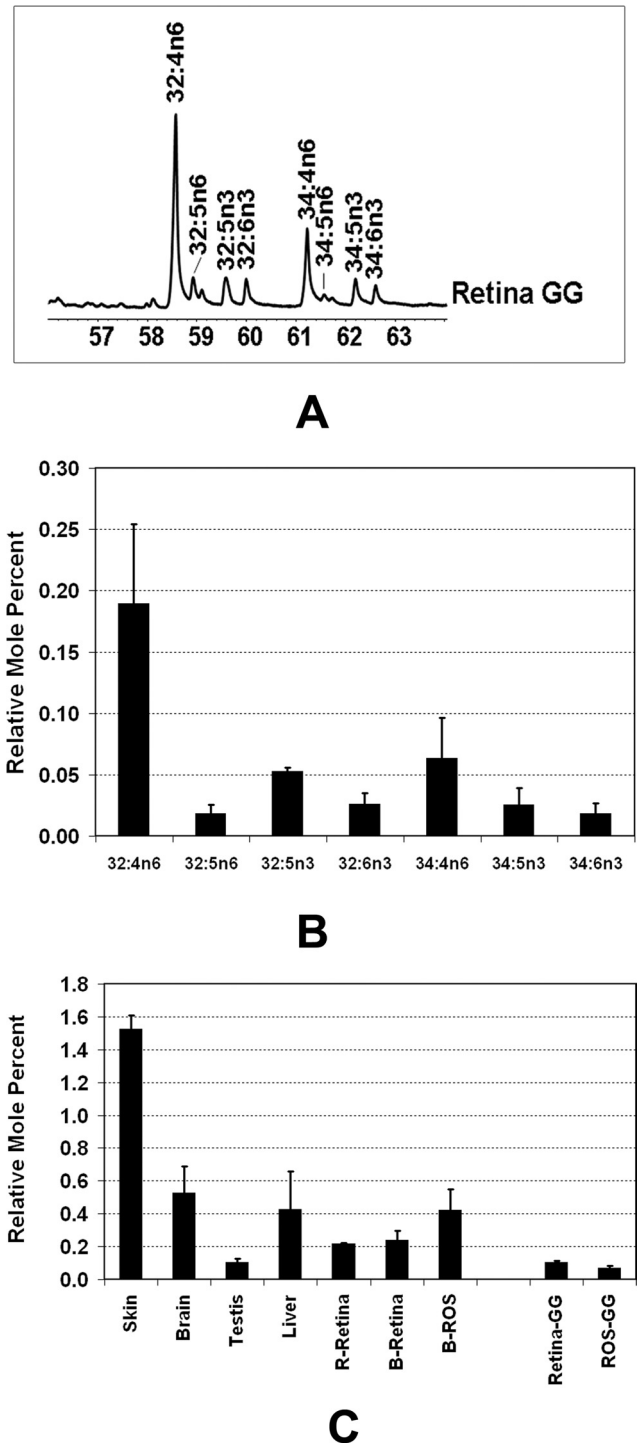

FIGURE 4. (**A**) Analysis of VLC-PUFAs of sialylated sphingolipids (i.e., GGs) by GC-MS. The PUFA response values were obtained by using the *m/z* ratios 79.1, 108.1, and 150.1 in SIM mode. (**B**) VLC-PUFA composition of bovine retinal GGs. The VLC-PUFAs were identified by GC-MS as shown in (**A**). The abundance was calculated from three independent samples after normalizing peak areas to the response of 22:0. (**C**) VLC-FA composition of sphingolipids. VLC-FA composition (sum of 26:0+28:0+30:0) in the NSL fraction of rat skin, brain, testis, liver, and retina (R-Retina), bovine retina (B-Retina), bovine ROS (B-ROS), and in the GG fraction of bovine retina (retina-GG) and bovine ROS (ROS-GG) are presented as mole percent of the total NSL and GG from the respective tissue/isolate (mean ± SD, $n = 3$). The group of seven bars at the *left* side of the chart represents mole percent of the total NSL fraction of tissue. The remaining two bars (*right*) represent the mole percent of the GG fractions.

CERs is available in the literature, except some compositional studies on retinal GGs.[49–53] In the present study, we characterized retinal CERs and GGs in terms of their abundance and fatty acid composition. We further extended our studies to characterize VLC-PUFA- and VLC-FA-containing sphingolipids in the retina for the first time, as recent publications from our and other groups indicate the importance of these lipids in retinal physiology and diseases.[30,31]

Besides the intrinsic difficulty of isolating and studying sphingolipids from any tissue, the other common hindrance is their low abundance. However, they are abundant in neural tissue such as the myelin sheath of brain, which contains ~30% sphingolipids (22% cerebroside and 8% SM) in the membrane.[54] We found the retinal fatty acids that belong to sphingolipids ranged from 6% to 7% of the total retinal fatty acid

pool. In comparison to phospholipids, the relative level of sphingolipids varied from 11 to 13 mole %, a high enough amount that sphingolipids can no longer be classified as a molecule of low abundance in the retina. It actually ranks as the third most abundant lipid in the retina after phospholipid and sterols.[40] It may be true that they are present in small quantities in other nonneuronal tissues, but can play important physiological roles. The sphingolipids, SMs, and GGs are enriched in membrane rafts and are involved in receptor functioning, cell–cell interaction and host–pathogen interaction. Cellular free CERs, on the other hand, are also very important for signaling. CER and its component SP, promote cell death, whereas their phosphorylated derivatives, C1P and S1P, respectively, promote cell survival, migration, and differentiation.[7] Therefore, the level of free CER is very tightly controlled in any cell. We found that the retinal content of free CERs is 15% to 18% of the total NSLs (Fig. 2B). At even low levels, when involved in signaling, the bioactive sphingolipids can play a major role, as exemplified by other classic signaling lipids such as phosphoinositides.[55–57]

NSLs from pig retinas were analyzed by Dreyfus et al.[51] by HPTLC. They used various types of HPTLC with a different solvent system to isolate and identify all the components of the retinal NSLs. Some of our unidentified GCs in Figure 2A were identified as mono-, di- and tri-hexosyl CERs by Dreyfus et al.[51] Although they determined the relative abundance of each species by densitometry, we determined the relative abundance by measuring the nanomoles or micrograms of fatty acid from each species by GC-FID. Our estimation of the relative abundance of SM to the total NSL was much higher than their estimation (70% vs. 35%). We verified our estimation by isolating SM by 2D HPTLC and by extracting total NSL with solid-phase extraction procedures. Our determination of the relative abundance of SM remained the same, regardless of the method of analysis.

There is no report on detailed fatty acid composition of retinal NSL thus far. After categorizing the retinal NSLs into seven CER classes, we determined the fatty acid composition of total NSL and each of the NSL fractions. At the same time, for a comparative study, we determined fatty acid compositions of NSLs in brain, liver, skin, and testis. What appears to be unique in retinal NSL fatty acid composition is the level of saturated fatty acids. Retinal NSLs contain the highest levels of saturated fatty acids (90%) among all the tissues tested, with 18:0 and 16:0 being the two major species (63% and 11%, respectfully; Table 1). The composition of free retinal CERs (S1, S2, and S3) was also very similar, of which 18:0+16:0 accounts for 64% to 76% (Table 3). This estimation matches closely the estimation by Fox et al.,[16] who reported that rat retinal CER contains 79% 16:0+18:0. Also, our measurement of the 16:0+18:0 composition in glucosyl CER species (62%–69%; Table 3, S4, S5, and S6) matches very closely the reported values of 63% to 70%.[16] The SM fraction, on the other hand, contributed >70% of total retinal NSL and contained >96% saturated FA (Table 3). SM in other tissues is known to contain higher quantities of unsaturated FAs, especially in testis,[44] but a composition of exclusive saturates in the retina may have some physiological importance. On the other hand, retinal levels of unsaturated amide-linked fatty acids are very low. The retinal value is the lowest of all tissues for n6 fatty acids, which is >10 times lower than skin. Among the polyunsaturated fatty acids, DHA contributes half of the total of only 4% in the retinal NSL. This finding is not surprising, since retinal ROS membranes possess some of the highest levels of DHA of any mammalian cells.[40] Low levels of amide-linked unsaturated fatty acids in the retina may indicate that NSL metabolic pools are different from phospholipid metabolic pools.

Another striking observation is the absence of VLC-PUFA (>26 carbons) in retinal NSL. Total retina contains a significant level of VLC-PUFAs (one of the highest in any mammalian tissue)[28,42,58] and very little VLC-FAs (Mandal et al., unpublished data, 2009). From studies in mouse models, we and others have reported that mice deficient in ELOVL4 protein lack VLC-FA-containing sphingolipids in the skin.[29–31] We have further discovered the involvement of ELOVL4 protein in specific biosynthetic steps of both VLC-FA and VLC-PUFA.[28] Stargardt 3 patients do not have any skin disease, and as the retina contains significant amounts of VLC-PUFAs, we speculate that retinal NSL contains a higher quantity of amide-bound VLC-PUFAs. However, we did not detect any amide-bound VLC-PUFAs beyond 24 carbons in the retinal NSL. Testis is another tissue with high levels of PUFAs and has significant membrane biogenesis comparable to retinal photoreceptors, the outer segments of which are renewed every 10 days.[59,60] We detected a fourfold higher level of unsaturated fatty acids (≤24 carbons; Table 1) in testis NSLs compared with retina. NSLs with VLC-PUFAs have been reported in the testis and specifically in the sperm head.[44,45] We used testis as a positive control in our VLC-PUFA analysis and confirmed the previous observations that testis indeed contain higher levels of VLC-PUFA-containing sphingolipids (Fig. 3).

However, retina contains ~200 picomoles of VLC-FAs per nanomole of TFAs, twofold higher than that found in the testis. These are also derived from activity of the ELOVL4 enzyme, and therefore it is possible that VLC-FA-containing CERs are involved in some specific function of the photoreceptor, with a defect in their biosynthesis causing retinal pathogenesis, much like that observed in the skin of *Elovl4* mice.[29–31] It also possible that STGD3 retinal disease is related to PUFA content of other lipid classes, such as PC.

The presence of SM has been reported in retinal ROS from rat, frog, bovine, human, and goldfish. The relative abundance was in the range of 0.7% in rat, 1.1% in bovine, 1.8% in human, and 3.1% in goldfish retina.[40] We detected 0.8 to 1.4 mole % NSLs in the bovine ROS, 70% to 80% of which belongs to SMs. We determined the fatty acid composition of this ROS NSL for the first time and found that ROS NSL was composed of 99% saturated fatty acids, with 18:0 (68%) and 16:0 (17%) being the major species with traces of VLC-FAs (Fig. 4B).

Although there are many reports on characterization of retinal GGs,[49–53] limited information is available on their fatty acid composition. In contrast to retinal NSLs, GGs are composed of significantly higher levels of unsaturated fatty acids with significant contribution from long-chain n6 and n3 PUFAs, such as arachidonic acid and DHA, which is very similar to the major retinal phospholipids[40] (Table 2). It could be the case that biosynthetic processes of NSLs and GGs are different and therefore they have different pools of fatty acids. Addition of sugars to the head group of GGs takes place in the Golgi, similar to the head group modification of other phospholipids, and therefore they probably follow a similar biosynthetic route, as suggested by their fatty acid composition. The pattern of GG distribution in retina is very similar to that of brain (Table 2). GG from ROS was also similar (Table 2). It could be true that the GG fatty acid pattern is similar in all neural tissues; this possibility should be verified by analyzing other neural and nonneural tissues. Another interesting finding regarding retinal GG fatty acid composition is the presence of VLC-PUFAs. As discussed earlier, the GG fatty acid composition is very similar to the composition of total retina, having higher levels of unsaturated fatty acids. Retinal PC is known to contain high levels of VLC-PUFAs[41,42] and therefore the presence of VLC-PUFAs in the GG fraction is not surprising; but, this is an important finding in terms of functionality of the ELOVL4 enzyme in the retina. If a particular class of lipid is responsible

for the ELOVL4 mutation-mediated retinal pathogenesis, the VLC-FA-containing NSL or the VLC-PUFA-containing GGs or both could be potential candidates.

The role of CER and its other bioactive metabolites in signaling for cell death and survival has now been well established. Recent studies revealed their involvement in photoreceptor cell death and inflammation and angiogenesis at photoreceptor-RPE interface.[21–23] Our comprehensive characterization of retinal sphingolipids lays the groundwork for future studies on the functional role of sphingolipids in the retina in normal physiology and disease.

Acknowledgments

The authors thank Yoshikazu Uchida (Department of Dermatology, School of Medicine, University of California San Francisco) for help in establishing some of the analytical procedures and Mark Dittmar and Alicia Avila (Dean A. McGee Eye Institute, Oklahoma City, OK) for assistance with animal breeding and feeding.

References

1. Martin RE, Elliott MH, Brush RS, Anderson RE. Detailed characterization of the lipid composition of detergent-resistant membranes from photoreceptor rod outer segment membranes. *Invest Ophthalmol Vis Sci.* 2005;46:1147–1154.
2. Gulbins E, Kolesnick R. Raft ceramide in molecular medicine. *Oncogene.* 2003;22:7070–7077.
3. Tsui-Pierchala BA, Encinas M, Milbrandt J, Johnson EM Jr. Lipid rafts in neuronal signaling and function. *Trends Neurosci.* 2002; 25:412–417.
4. Michel V, Bakovic M. Lipid rafts in health and disease. *Biol Cell.* 2007;99:129–140.
5. Huwiler A, Kolter T, Pfeilschifter J, Sandhoff K. Physiology and pathophysiology of sphingolipid metabolism and signaling. *Biochim Biophys Acta.* 2000;1485:63–99.
6. Hannun YA, Luberto C. Lipid metabolism: ceramide transfer protein adds a new dimension. *Curr Biol.* 2004;14:R163–R165.
7. Hannun YA, Obeid LM. Principles of bioactive lipid signalling: lessons from sphingolipids. *Nat Rev.* 2008;9:139–150.
8. Levade T, Malagarie-Cazenave S, Gouaze V, et al. Ceramide in apoptosis: a revisited role. *Neurochem Res.* 2002;27:601–607.
9. Riboni L, Bassi R, Anelli V, Viani P. Metabolic formation of ceramide-1-phosphate in cerebellar granule cells: evidence for the phosphorylation of ceramide by different metabolic pathways. *Neurochem Res.* 2002;27:711–716.
10. Riboni L, Campanella R, Bassi R, et al. Ceramide levels are inversely associated with malignant progression of human glial tumors. *Glia.* 2002;39:105–113.
11. Litvak DA, Bilchik AJ, Cabot MC. Modulators of ceramide metabolism sensitize colorectal cancer cells to chemotherapy: a novel treatment strategy. *J Gastrointest Surg.* 2003;7:140–148; discussion 148.
12. Buccoliero R, Futerman AH. The roles of ceramide and complex sphingolipids in neuronal cell function. *Pharmacol Res.* 2003;47: 409–419.
13. Ferlinz K, Hurwitz R, Sandhoff K. Molecular basis of acid sphingomyelinase deficiency in a patient with Niemann-Pick disease type A. *Biochem Biophys Res Commun.* 1991;179:1187–1191.
14. Ainsworth PJ, Coulter-Mackie MB. A double mutation in exon 6 of the beta-hexosaminidase alpha subunit in a patient with the B1 variant of Tay-Sachs disease. *Am J Hum Genet.* 1992;51:802–809.
15. Blanch LC, Meaney C, Morris CP. A sensitive mutation screening strategy for Fabry disease: detection of nine mutations in the alpha-galactosidase A gene. *Hum Mutat.* 1996;8:38–43.
16. Fox TE, Han X, Kelly S, et al. Diabetes alters sphingolipid metabolism in the retina: a potential mechanism of cell death in diabetic retinopathy. *Diabetes.* 2006;55:3573–3580.
17. Hartong DT, Berson EL, Dryja TP. Retinitis pigmentosa. *Lancet.* 2006;368:1795–1809.
18. Haddad S, Chen CA, Santangelo SL, Seddon JM. The genetics of age-related macular degeneration: a review of progress to date. *Surv Ophthalmol.* 2006;51:316–363.
19. Allikmets R. Leber congenital amaurosis: a genetic paradigm. *Ophthalmic Genet.* 2004;25:67–79.
20. Glazer LC, Dryja TP. Understanding the etiology of Stargardt's disease. *Ophthalmol Clin North Am.* 2002;15:93–100,viii.
21. German OL, Miranda GE, Abrahan CE, Rotstein NP. Ceramide is a mediator of apoptosis in retina photoreceptors. *Invest Ophthalmol Vis Sci.* 2006;47:1658–1668.
22. Acharya U, Patel S, Koundakjian E, Nagashima K, Han X, Acharya JK. Modulating sphingolipid biosynthetic pathway rescues photoreceptor degeneration. *Science.* 2003;299:1740–1743.
23. Xie B, Shen J, Dong A, Rashid A, Stoller G, Campochiaro PA. Blockade of sphingosine-1-phosphate reduces macrophage influx and retinal and choroidal neovascularization. *J Cell Physiol.* 2009; 218:192–198.
24. Skoura A, Sanchez T, Claffey K, Mandala SM, Proia RL, Hla T. Essential role of sphingosine 1-phosphate receptor 2 in pathological angiogenesis of the mouse retina. *J Clin Invest.* 2007;117: 2506–2516.
25. Ali M, Ramprasad VL, Soumittra N, et al. A missense mutation in the nuclear localization signal sequence of CERKL (p.R106S) causes autosomal recessive retinal degeneration. *Mol Vis.* 2008;14: 1960–1964.
26. Auslender N, Sharon D, Abbasi AH, Garzozi HJ, Banin E, Ben-Yosef T. A common founder mutation of CERKL underlies autosomal recessive retinal degeneration with early macular involvement among Yemenite Jews. *Invest Ophthalmol Vis Sci.* 2007;48:5431–5438.
27. Tuson M, Marfany G, Gonzalez-Duarte R. Mutation of CERKL, a novel human ceramide kinase gene, causes autosomal recessive retinitis pigmentosa (RP26). *Am J Hum Genet.* 2004;74:128–138.
28. Agbaga MP, Brush RS, Mandal MN, Henry K, Elliott MH, Anderson RE. Role of Stargardt-3 macular dystrophy protein (ELOVL4) in the biosynthesis of very long chain fatty acids. *Proc Natl Acad Sci U S A.* 2008;105:12843–12848.
29. Li W, Sandhoff R, Kono M, et al. Depletion of ceramides with very long chain fatty acids causes defective skin permeability barrier function, and neonatal lethality in ELOVL4 deficient mice. *Int J Biol Sci.* 2007;3:120–128.
30. McMahon A, Butovich IA, Mata NL, et al. Retinal pathology and skin barrier defect in mice carrying a Stargardt disease-3 mutation in elongase of very long chain fatty acids-4. *Mol Vis.* 2007;13:258–272.
31. Vasireddy V, Uchida Y, Salem N Jr, et al. Loss of functional ELOVL4 depletes very long-chain fatty acids (> or = C28) and the unique omega-O-acylceramides in skin leading to neonatal death. *Hum Mol Genet.* 2007;16:471–482.
32. Papermaster DS, Dreyer WJ. Rhodopsin content in the outer segment membranes of bovine and frog retinal rods. *Biochemistry.* 1974;13:2438–2444.
33. Bligh EG, Dyer WJ. A rapid method of total lipid extraction and purification. *Can J Biochem Physiol.* 1959;37:911–917.
34. Martin RE. Docosahexaenoic acid decreases phospholipase A2 activity in the neurites/nerve growth cones of PC12 cells. *J Neurosci Res.* 1998;54:805–813.
35. Rouser G, Siakotos AN, Fleischer S. Quantitative analysis of phospholipids by thin-layer chromatography and phosphorus analysis of spots. *Lipids.* 1966;1:85–86.
36. Bodennec J, Famy C, Brichon G, Zwingelstein G, Portoukalian J. Purification of free sphingoid bases by solid-phase extraction on weak cation exchanger cartridges. *Anal Biochem.* 2000;279:245–248.
37. Ladisch S, Li R. Purification and analysis of gangliosides. *Methods Enzymol.* 2000;312:135–145.
38. Uchida Y, Hara M, Nishio H, et al. Epidermal sphingomyelins are precursors for selected stratum corneum ceramides. *J Lipid Res.* 2000;41:2071–2082.
39. Ford DA, Monda JK, Brush RS, Anderson RE, Richards MJ, Fliesler SJ. Lipidomic analysis of the retina in a rat model of Smith-Lemli-Opitz syndrome: alterations in docosahexaenoic acid content of

phospholipid molecular species. *J Neurochem.* 2008;105:1032–1047.

40. Fliesler SJ, Anderson RE. Chemistry and metabolism of lipids in the vertebrate retina. *Prog Lipid Res.* 1983;22:79–131.
41. Aveldano MI, Sprecher H. Very long chain (C24 to C36) polyenoic fatty acids of the n-3 and n-6 series in dipolyunsaturated phosphatidylcholines from bovine retina. *J Biol Chem.* 1987;262:1180–1186.
42. Aveldano MI. A novel group of very long chain polyenoic fatty acids in dipolyunsaturated phosphatidylcholines from vertebrate retina. *J Biol Chem.* 1987;262:1172–1179.
43. Poulos A. Very long chain fatty acids in higher animals: a review. *Lipids.* 1995;30:1–14.
44. Furland NE, Oresti GM, Antollini SS, Venturino A, Maldonado EN, Aveldano MI. Very long-chain polyunsaturated fatty acids are the major acyl groups of sphingomyelins and ceramides in the head of mammalian spermatozoa. *J Biol Chem.* 2007;282:18151–18161.
45. Furland NE, Zanetti SR, Oresti GM, Maldonado EN, Aveldano MI. Ceramides and sphingomyelins with high proportions of very long-chain polyunsaturated fatty acids in mammalian germ cells. *J Biol Chem.* 2007;282:18141–18150.
46. Brady RO. Sphingolipid metabolism in neural tissues. *Neurosci Res.* 1969;2:301–315.
47. Colombaioni L, Garcia-Gil M. Sphingolipid metabolites in neural signalling and function. *Brain Res.* 2004;46:328–355.
48. Uchida Y, Holleran WM. Omega-O-acylceramide, a lipid essential for mammalian survival. *J Dermatol Sci.* 2008;51:77–87.
49. Edel-Harth S, Dreyfus H, Bosch P, Rebel G, Urban PF, Mandel P. Gangliosides of whole retina and rod outer segments. *FEBS Lett.* 1973;35:284–288.
50. Holm M, Mansson JE. Differences in sphingosine and fatty acid patterns of the major gangliosides of bovine retina. *FEBS Lett.* 1974;38:261–262.
51. Dreyfus H, Guerold B, Freysz L, Hicks D. Successive isolation and separation of the major lipid fractions including gangliosides from single biological samples. *Anal Biochem.* 1997;249:67–78.
52. Fontaine V, Hicks D, Dreyfus H. Changes in ganglioside composition of photoreceptors during postnatal maturation of the rat retina. *Glycobiology.* 1998;8:183–190.
53. Dreyfus H, Guerold B, Fontaine V, Sahel J, Hicks D. Simplified ganglioside composition of photoreceptors compared to other retinal neurons. *Invest Ophthalmol Vis Sci.* 1996;37:574–585.
54. Morell P, Quarles R H. Myelin formation, structure and biochemistry. In: Siegel GJ, Agranoff BW, Albers RW, Fisher SK, Uhler, MD, eds. *Basic Neurochemistry Molecular*, *Cellular*, *and Medical Aspects.* Philadelphia: Lippincott-Raven; 1999:51–71.
55. Brown JE, Rubin LJ, Ghalayini AJ, et al. myo-Inositol polyphosphate may be a messenger for visual excitation in Limulus photoreceptors. *Nature.* 1984;311:160–163.
56. Duronio V. The life of a cell: apoptosis regulation by the PI3K/PKB pathway. *Biochem J.* 2008;415:333–344.
57. Yuan TL, Cantley LC. PI3K pathway alterations in cancer: variations on a theme. *Oncogene.* 2008;27:5497–5510.
58. Aveldano MI. Long and very long polyunsaturated fatty acids of retina and spermatozoa: the whole complement of polyenoic fatty acid series. *Adv Exp Med Biol.* 1992;318:231–242.
59. LaVail MM. Kinetics of rod outer segment renewal in the developing mouse retina. *J Cell Biol.* 1973;58:650–661.
60. LaVail MM. Rod outer segment disk shedding in rat retina: relationship to cyclic lighting. *Science.* 1976;194:1071–1074.